Carbohydrate Research, 246 (1993) 43–49
Elsevier Science Publishers B.V., Amsterdam

Mapping of the spatial variation in alginate concentration in calcium alginate gels by magnetic resonance imaging (MRI)

Kimberlee Potter, T. Adrian Carpenter and Laurance D. Hall

Herchel Smith Laboratory for Medicinal Chemistry, Cambridge University School of Clinical Medicine, University Forvie Site, Robinson Way, Cambridge CB2 2PZ (United Kingdom)

(Received November 26th, 1992; accepted March 8th, 1993)

ABSTRACT

A series of homogeneous calcium alginate gels, prepared in the presence of anti-gelling ions, were used to produce a calibration curve relating the spin–spin relaxation time (T_2) of the water protons in the gel to the concentration of alginate. This was then used to calculate the spatial variation of alginate concentration in an inhomogeneous calcium alginate gel from a T_2 map computed from a series of one-dimensional MR-projection images. The concentration gradient for alginate derived thereby compared favourably with that subsequently obtained by physical sectioning of the gel.

INTRODUCTION

Calcium alginate, produced by the diffusion of calcium ions into an aqueous solution of sodium alginate, forms a spatially inhomogeneous gel in which there is a higher concentration of alginate in the region which first comes in contact with the calcium ions. This heterogeneity has already been investigated by physical sectioning of the sample followed by gravimetric analysis of the slices[1], and also visualised directly by one-, two-, and three-dimensional magnetic resonance imaging (MRI) for different geometries[2].

In this paper we report, for an inhomogeneous slab of calcium alginate, the dependence of the spin–spin relaxation times (T_2) of the water protons within the gel on alginate concentration. Measurement of a series of homogeneous gels of various alginate concentrations gave an equation which relates alginate concentration to the T_2 of the water protons within the gel. When applied to the T_2 image of an inhomogeneous calcium alginate gel, that relationship gives a map of alginate concentration as a function of distance along the axis of the gel. The derived alginate concentration gradient is similar to that obtained by physical sectioning of the gel.

RESULTS AND DISCUSSION

A one-dimensional T_2 map of an inhomogeneous calcium alginate slab, made from an aqueous 2% (w/v) solution of sodium alginate[3], was calculated from a series of one-dimensional MR-projections taken parallel to the axis of the gel for different echo times and fitting the results to a single exponential decay curve of the form:

$$M = M_0 \exp(-TE/T_2) + \text{constant}. \quad (1)$$

The proton density (M_0) and the T_2 profiles of the gel are given in Figs. 1(a) and 1(b), respectively. Note that the proton density map Fig. 1(a) does not exactly represent the number of water protons present in the gel; rather it shows the relative distribution of the water protons within the gel. When Fig. 1(a) is viewed from left to right, the water content of the gel increases, which implies that the

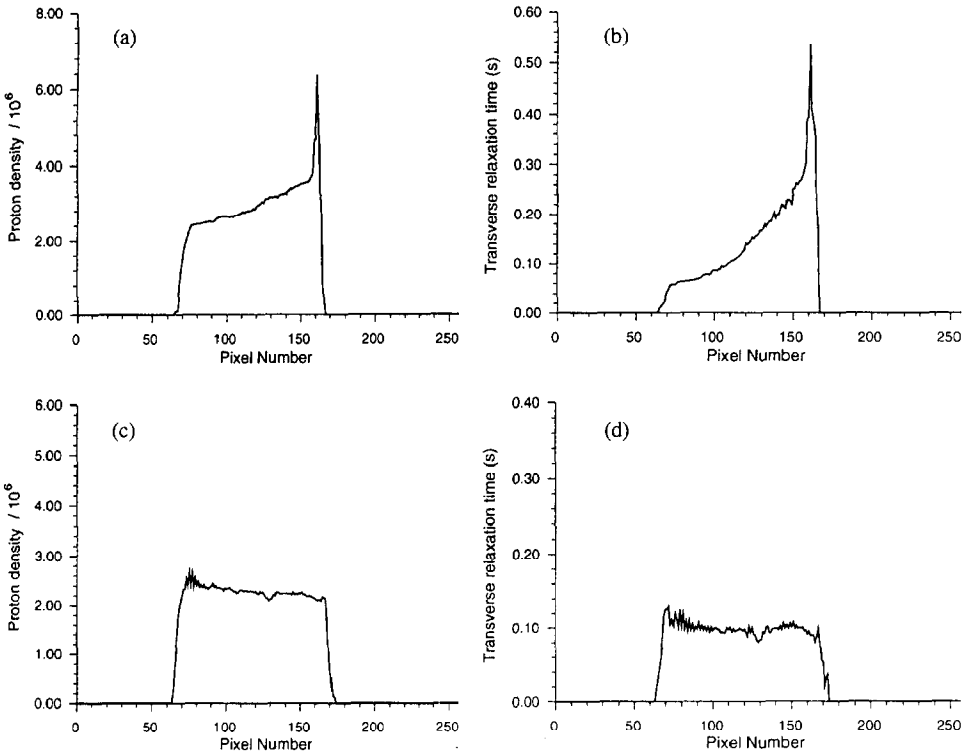

Fig. 1. (a) A one-dimensional proton density (M_0) map of an inhomogeneous calcium alginate slab; (b) a one-dimensional map of the T_2 values of the water protons in the same gel; (c) a one-dimensional proton density map of a homogeneous calcium alginate slab; and (d) a one-dimensional map of the T_2 values of the water protons in the same gel. The direction of gel formation was from left to right and the pixel resolution was 160 μm.

TABLE I

Results of physical sectioning experiment of an inhomogeneous calcium alginate gel

Slice No.	Alginate content (w/w%)	T_1 (s)	T_2 (s)
1	4.3	1.5 (0.02) [a]	0.053 (0.0002)
2	2.9	1.6 (0.02)	0.069 (0.0001)
3	1.7	1.7 (0.03)	0.095 (0.0008)
4	1.4	1.8 (0.02)	0.122 (0.001)
5	1.7	1.7 (0.02)	0.145 (0.002)

[a] The value shown in brackets is the error in the fit of the curve to the experimental data.

alginate content decreases; the T_2 values [Fig. 1(b)] also increase from left to right, which suggests that T_2 varies inversely with alginate concentration.

To verify the dependence of T_2 on alginate concentration, the same calcium alginate slab was then sectioned into 5 slices (each ~ 3 mm thick), parallel to the direction of gel formation; the bulk T_1 (measured by inversion recovery[4]) and the bulk T_2 (measured using a Carr–Purcell–Melboom–Gill (CPMG) spin-echo sequence[5]) for each slice were then determined. The slices were then dried in an oven overnight and the percent dry weight was recorded as the percentage of alginate (w/w%) contained in each slice (Table I); the first slice, labelled No. 1, corresponds to the gel which is formed when sodium alginate solution first comes in contact with calcium ions.

The results presented in Table I demonstrate that T_2 of the water proton in the gel varies with alginate concentration, whereas T_1 does not differ significantly from bulk water. It should be noted that the percentage of alginate (w/w%) measured gravimetrically is not very precise as it is impossible to remove all the associated water[6]; other sources of error include water loss both when the gel is sliced and also during the measurement of the proton relaxation times, as well as the presence of associated ions.

In order to investigate further the T_2-dependence of the water protons on alginate concentration, it was necessary to fabricate gels which were homogeneous and contained a known amount of alginate. Those homogeneous gels were produced by the addition of anti-gelling ions[1] and the degree of homogeneity was verified by plotting the M_0 and T_2 profiles of the water protons within each of the gels. Both the water proton density map [Fig. 1(c)] and the T_2 map [Fig. 1(d)] of a typical homogeneous calcium alginate gel, made using the same sodium alginate concentration as for the inhomogeneous slab (2% w/v), were quite uniform.

The bulk T_1 and T_2 values of the water protons within that series of homogeneous gels were measured and the results are recorded in Table II. The plot of $1/T_2$ against alginate concentration (w/v%) was linear (Fig. 2); similar linear relationships have been observed in other systems, such as agarose[7], bovine serum albumin[8], and agar[9]. Importantly, it provides a unique way in which to obtain information about gel concentration without destroying the gel itself. Clearly, the

TABLE II

Bulk relaxation times for a series of homogeneous calcium alginate gels

Alginate content (w/v%)	T_1 (s)	T_2 (s)
1.0	2.11 (0.03) [a]	0.211 (0.0003)
1.5	2.16 (0.01)	0.151 (0.0001)
2.0	1.92 (0.01)	0.110 (0.0002)
2.5	2.01 (0.01)	0.094 (0.0001)
3.0	1.88 (0.01)	0.084 (0.0002)

[a] The value shown in brackets is the error in the fit of the curve to the experimental data.

accuracy of this relationship is dependent on the accuracy to which the alginate content of the gel can be measured; in this study, the concentration of the sodium alginate solution used in the fabrication of the gel was taken to be a measure of the concentration of alginate within the gel.

According to the theory of water proton relaxation times in polysaccharide gels[10,11], provided that the scale of the heterogeneities within the gel are such that the properties of the water can be diffusion-averaged, the main mechanism for relaxation is by chemical exchange with the hydroxyl protons of the polysaccharide molecule. This is the case for alginate gels since the pore sizes determined by electron microscopy[12] are of the order of 20–200 nm, which is well within the 'fast diffusion' limit.

If that hypothesis is correct, then the T_2 of the water protons within the gel is a complex function of the number of exchangeable protons on the polysaccharide, the rate of exchange with those sites (k_g^{-1}), and the T_2 of the protons at those exchangeable sites (T_{2g}). Although it is difficult to measure any one of those parameters with any degree of accuracy, it is possible to relate the number of exchangeable protons to the polysaccharide concentration; thus,

$$[1/T_2]_{obsd} = [1/T_2]_{bulk} + K[\text{alginate}]/\left[T_{2g} + k_g^{-1}\right] \quad (2)$$

where K is a constant relating the concentration of alginate to the number of exchangeable protons.

From the graph shown in Fig. 2, it can be seen that at zero alginate concentration the observed T_2 ($\sim$ 800 ms) corresponds to the T_2 of water protons in a dilute solution of sodium alginate; this suggests that the interstitial spaces in the gel do not contain pure water, but also some dissolved alginate molecules. The slope of the graph cannot be analysed in terms of the various contributions because of the many unknowns; however, the derived slope is unique for this system, since it depends on the polysaccharide involved, the rate of chemical exchange (which is also temperature dependent), and how the alginate concentration is defined. The effect of alginate concentration on the T_1 of the water protons within the gel (Table II) is not significant, since the T_1 of the exchangeable protons is not very much different to that of bulk water.

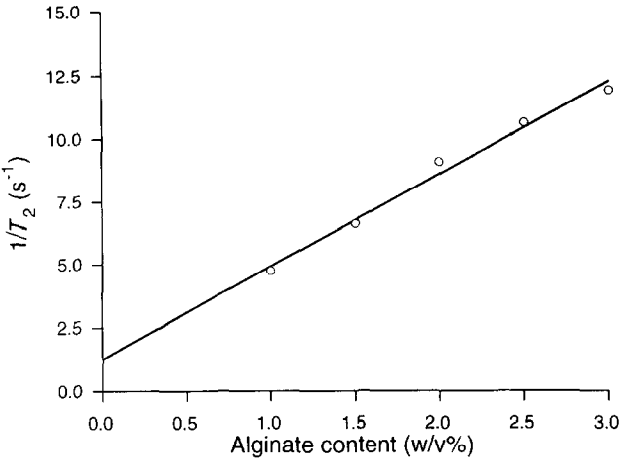

Fig. 2. Plot of $1/T_2$ (s^{-1}) vs. alginate content (w/v%) for a series of homogeneous alginate gels. The slope of the fitted straight line was 3.67 and the intercept was 1.26 s^{-1}.

Equation *2* was then applied to the T_2 map of an inhomogeneous calcium alginate gel [Fig. 1(b)] to give a map of alginate concentration as a function of distance along the axis of the gel. These results are plotted in Fig. 3 together with the results from the physical sectioning experiment. Allowing for the poorer resolution of the physical sectioning experiment, it was found that the concentration of alginate in each slice compared favourably with the concentration of alginate averaged over the thickness of the slice (~ 3 mm) in the concentration map (Fig. 3). For slices 2 and 3, the alginate content is underestimated and in slice

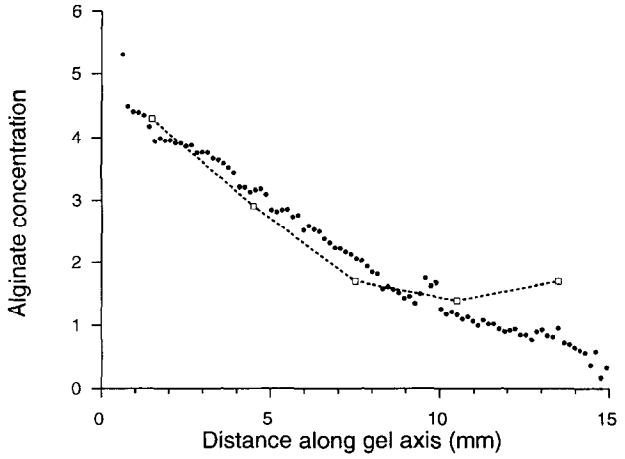

Fig. 3. The discrete points show the variation in alginate concentration along the axis of an inhomogeneous calcium alginate slab, derived from the T_2 map of this gel [Fig. 1(b)]. The open squares joined by a dashed line (- - - - -) give the results of the physical sectioning experiment; the alginate concentration of each slice is plotted at the position corresponding to the middle of the slice.

5 it is overestimated; this may reflect the fact that the inner slices tend to have more water associated with them, so that the weight loss on drying is greater than for the outer slices which are already partly dried because of exposure to the air.

Based on the above results, it is now possible to use MRI to map alginate concentration gradients within calcium alginate gels without destroying them. Since the concentration of alginate determines the pore size[13] of the gel matrix, those concentration maps will be useful for mapping the distribution of pore sizes within the gel, which has important applications in such fields as agriculture[14] and medicine[15] where the controlled release of small molecules is required. The large reduction in the T_2 of water protons, which accompanies the transition from sol to gel, provides an elegant means of tracking the displacement of the sol–gel interface. This will enable us to study the kinetics of the gelation process and thereby gain further insight into the physio-chemical properties of calcium alginate gels.

EXPERIMENTAL

Inhomogeneous gels.—An inhomogeneous calcium alginate slab[3] was fabricated by pouring an aq 2% (w/v) solution of sodium alginate (Fisons) into a plastic cylinder (i.d. 32 mm, height 24 mm) with a dialysis membrane (Medicell International Ltd.) at one end, and dialysing against 0.06 M $CaCl_2 \cdot 6H_2O$ (Fisons A.R. Grade).

Homogeneous gels.—Homogeneous calcium alginate gels (1.0, 1.5, 2.0, 2.5, and 3.0 w/v%) were made by dissolving sodium alginate in 0.2 M NaCl (Fisons A.R. Grade) followed by dialysis against 0.06 M $CaCl_2$[1].

MRI instrumentation.—All MRI experiments were conducted using an Oxford Research Systems BIOSPEC I imaging-spectrometer coupled to an Oxford Instruments 310-mm horizontal bore, superconducting magnet operating at 2.0 T (83.7 MHz for ^1H). Magnetic field gradients for imaging in three orthogonal directions were generated by a custom built Helmholtz–Golay gradient set[16] (i.d. 200 mm), and all samples were studied using a split-ring resonator probe[17] (i.d. 60 mm, height 115 mm) placed with its long axis vertical in the bore of the gradient set.

Relaxation studies.—Bulk T_1 measurements were made using inversion recovery[4], and bulk T_2 measurements were made using a CPMG pulse sequence[5].

One-dimensional imaging.—One-dimensional projection images of alginate slabs in air were obtained using a Hahn spin-echo sequence[18]. with variable echo times (TE = 20, 30,..., 170 ms), in the presence of a pulsed magnetic field gradient (1.2 Gauss/cm) oriented perpendicular to the alginate slab. Each projection image represents a 4-cm field of view, resulting in a spatial resolution of 160 μm along the cylindrical axis of the slab.

These projections were then fitted to a single exponential decay curve of the form:

$$M = M_0 \exp(-TE/T_2) + \text{constant},$$

and the values of M_0 and T_2 were extracted for various positions along the axis of the slab (Fig. 1).

Computing.—All image data were processed on a Sun 4/150 TAAC workstation, using in-house "CaMReS" software (written by Dr. Nick Herrod). Relaxation data were fitted using in-house software (written by Dr. John Attard) based on the Levenburg–Marquardt nonlinear least-squares minimisation algorithm[19].

ACKNOWLEDGMENTS

It is a pleasure to thank Dr. Herchel Smith for a munificent benefaction (L.D.H. and T.A.C.) and studentship (K.P.), and the ORS Award Scheme for additional financial support (K.P.). Drs. Bruce Balcom and Suzanne Duce provided helpful discussions, and Drs. Nick Herrod and John Attard the software used.

REFERENCES

1 G. Skjåk-Bræk, H. Grasdalen, and O. Smidsrød, *Carbohydr. Polym.*, 10 (1989) 31–54.
2 K. Potter, N.J. Herrod, T.A. Carpenter, and L.D. Hall, *Carbohydr. Res.*, 239 (1993) 249–256.
3 A. Martinsen, G. Skjåk-Bræk, and O. Smidsrød, *Biotechnol. Bioeng.*, 33 (1989) 79–89.
4 R.L. Vold, J.S. Waugh, M.P. Klein, and D.E. Phelps, *J. Chem. Phys.*, 48 (1968) 688–691.
5 S. Melboom and D. Gill, *Rev. Sci. Instr.*, 29 (1958) 688–691.
6 E. Percival and R.H. Macdowell, *Chemistry and Enzymology of Marine Algal Polysaccharides*, Academic Press, London, 1967, Chapter 5, pp 114.
7 W. Derbyshire and I.D. Duff, *Discuss. Faraday Soc.*, 57 (1974) 243–254.
8 B.P. Hills, S.F. Takacs, and P.S. Belton, *Mol. Phys.*, 67 (1989) 919–937.
9 S.L. Duce, T.A. Carpenter, and L.D. Hall, *Carbohydr. Res.*, 205 (1990) c1–c4.
10 P.S. Belton, B.P. Hills, and E. Raimbaud, *Mol. Phys.*, 63 (1988) 825–842.
11 B.P. Hills, K.M. Wright, and P.S. Belton, *Mol. Phys.*, 67 (1989) 1309–1326.
12 J. Klein, J. Stock, and K-D Vorlop, *Eur. J. Appl. Microbiol. Biotechnol.*, 18 (1983) 86–91.
13 H. Tanaka, M. Matsumura, and I.A. Veliky, *Biotechnol. Bioeng.*, 26 (1984) 53–58.
14 A.B. Pepperman, J.W. Kuan, and C. McCombs, *J. Controlled Release*, 17 (1991) 105–111.
15 C.J. Gray and J. Dowsett, *Biotechnol. Bioeng.*, 31 (1988) 607–612.
16 T.A. Carpenter, L.D. Hall, and P. Jezzard, *J. Magn. Reson.*, 84 (1989) 383–387.
17 L.D. Hall, T. Marcus, C. Neale, B. Powell, J. Sallos, and S.L. Talgala, *J. Magn. Reson.*, 62 (1985) 525–528.
18 E.L. Hahn, *Phys. Rev.*, 80 (1950) 580–594.
19 W.H. Press, S.A. Flannery, S.A. Teukolsky, and W.T. Vetterling, *Numerical Recipes in C: The Art of Scientific Computing*, Cambridge University Press, New York, 1988, Chapter 8.